



US007590273B2

(12) **United States Patent**  
**Kubota et al.**

(10) **Patent No.:** **US 7,590,273 B2**  
(45) **Date of Patent:** **Sep. 15, 2009**

(54) **ESTIMATION OF SOLITARY PULMONARY NODULE DIAMETERS WITH A HYBRID SEGMENTATION APPROACH**

7,187,800 B2 \* 3/2007 Hibbard ..... 382/173  
2008/0137970 A1 \* 6/2008 Kubota ..... 382/224

**OTHER PUBLICATIONS**

(75) Inventors: **Toshiro Kubota**, Malvern, PA (US);  
**Kazunori Okada**, Plainsboro, NJ (US)

Estimating diameters of pulmonary nodules with competition diffusion and robust ellipsoid fit, Kubota et al, 2005.\*  
CT screening for lung cancer: Frequency and significance of part solid and non solid nodules, 2005.\*

(73) Assignees: **Siemens Corporate Research, Inc.**,  
Princeton, NJ (US); **Siemens Medical Solutions USA, Inc.**, Malvern, PA (US)

Three-Dimensional Segmentation and Growth-Rate Estimation of Small Pulmonary Nodules in Helical CT Images, 2003.\*

(\* ) Notice: Subject to any disclaimer, the term of this patent is extended or adjusted under 35 U.S.C. 154(b) by 702 days.

Binsheng Zhao, et al. "Automatic Detection of Small Lung Nodules on CT Utilizing a Local Density Maximum Algorithm" Journal of Applied Clinical Medical Physics, vol. 4, No. 3, Summer 2003, pp. 248-260.

(21) Appl. No.: **11/398,099**

Toshiro Kubota, et al. "Reaction-Diffusion Systems for Hypothesis Propagation", pp. 1-4, Sep. 2000.

(22) Filed: **Apr. 4, 2006**

Claudia I. Henschke, et al. "CT Screening for Lung Cancer: Frequency and Significance of Part-Solid and Nonsolid Nodules," AJR: 178, May 2002, pp. 1053-1057.

(65) **Prior Publication Data**

(Continued)

US 2006/0228013 A1 Oct. 12, 2006

*Primary Examiner*—Vikram Bali  
*Assistant Examiner*—Nancy Bitar

**Related U.S. Application Data**

(57) **ABSTRACT**

(60) Provisional application No. 60/669,438, filed on Apr. 8, 2005.

A method for estimating a diameter of an object of interest, includes extracting a sub-volume of voxels around a marker identifying a location of the object of interest, and determining a segmentation result identifying an edge of the object of interest by a reactive-diffusion method. The method further includes performing a boundary check on the segmentation result to determine whether the object of interest is solitary, estimating a diameter of the object of interest from the segmentation result upon determining the object of interest to be solitary, and extracting the object of interest by performing ellipsoid fit on the sub-volume and estimating a diameter of the object of interest upon determining the object of interest to be non-solitary.

(51) **Int. Cl.**  
**G06K 9/00** (2006.01)

(52) **U.S. Cl.** ..... **382/131**; 382/128; 382/173;  
382/224; 378/8; 378/62; 378/15; 378/901

(58) **Field of Classification Search** ..... 382/128,  
382/131, 173, 224; 378/62, 8, 15, 901

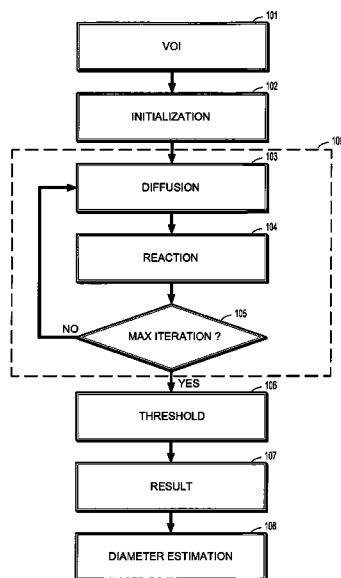
See application file for complete search history.

(56) **References Cited**

**U.S. PATENT DOCUMENTS**

5,936,628 A \* 8/1999 Kitamura et al. .... 345/420  
6,891,922 B2 \* 5/2005 Ferrant et al. .... 378/62

**13 Claims, 4 Drawing Sheets**



OTHER PUBLICATIONS

Okada et al., "Robust Anisotropic Gaussian Fitting for Volumetric Characterization of Pulmonary Nodules in Multislice CT", IEEE Transactions on Medical Imaging, IEEE Service Center, Piscataway, NJ, US, vol. 24, No. 3, Mar. 2005, pp. 409-423.

Kubota et al., "Reaction-diffusion Systems for Hypothesis Propagation", Pattern Recognition, 2000. Proceedings. 15<sup>th</sup> International Conference on Sep. 3-7, 2000, Los Alamitos, CA, USA, IEEE Comput. Soc, US, vol. 3, Sep. 3, 2000, pp. 543-546.

Rogowska, "Overview and Fundamentals of Medical Image Segmentation", Handbook of Medical Imaging Processing and Analysis, 2000, pp. 69-85.

Kostis et al., "Three-Dimensional Segmentation and Growth-Rate Estimation of Small Pulmonary Nodules in Helical CT Images",

IEEE Transactions on Medical Imaging, IEEE Service Center, Piscataway, NJ, US, vol. 22, No. 10, Oct. 2003, pp. 1259-1274.

Okada et al., "Robust 3D Segmentation of Pulmonary Nodules in Multislice CT Images", Lecture Notes in Computer Science, Springer Verlag, Berlin, DE, vol. 3217, Sep. 26, 2004, pp. 881-889.

Zhao et al., "Automatic Detection of Small Lung Nodules on CT Utilizing a Local Density Maximum Algorithm", Journal of Applied Clinical Medical Physics, American College of Medical Physics, Melville, NY, US, vol. 4, No. 3, Jul. 2003, pp. 248-260.

Tek et al., "Volumetric Segmentation of Medical Images by Three-Dimensional Bubbles", Computer Vision and Image Understanding, Academic Press, San Diego, CA, US, vol. 65, No. 2, Feb. 1997, pp. 246-258.

\* cited by examiner

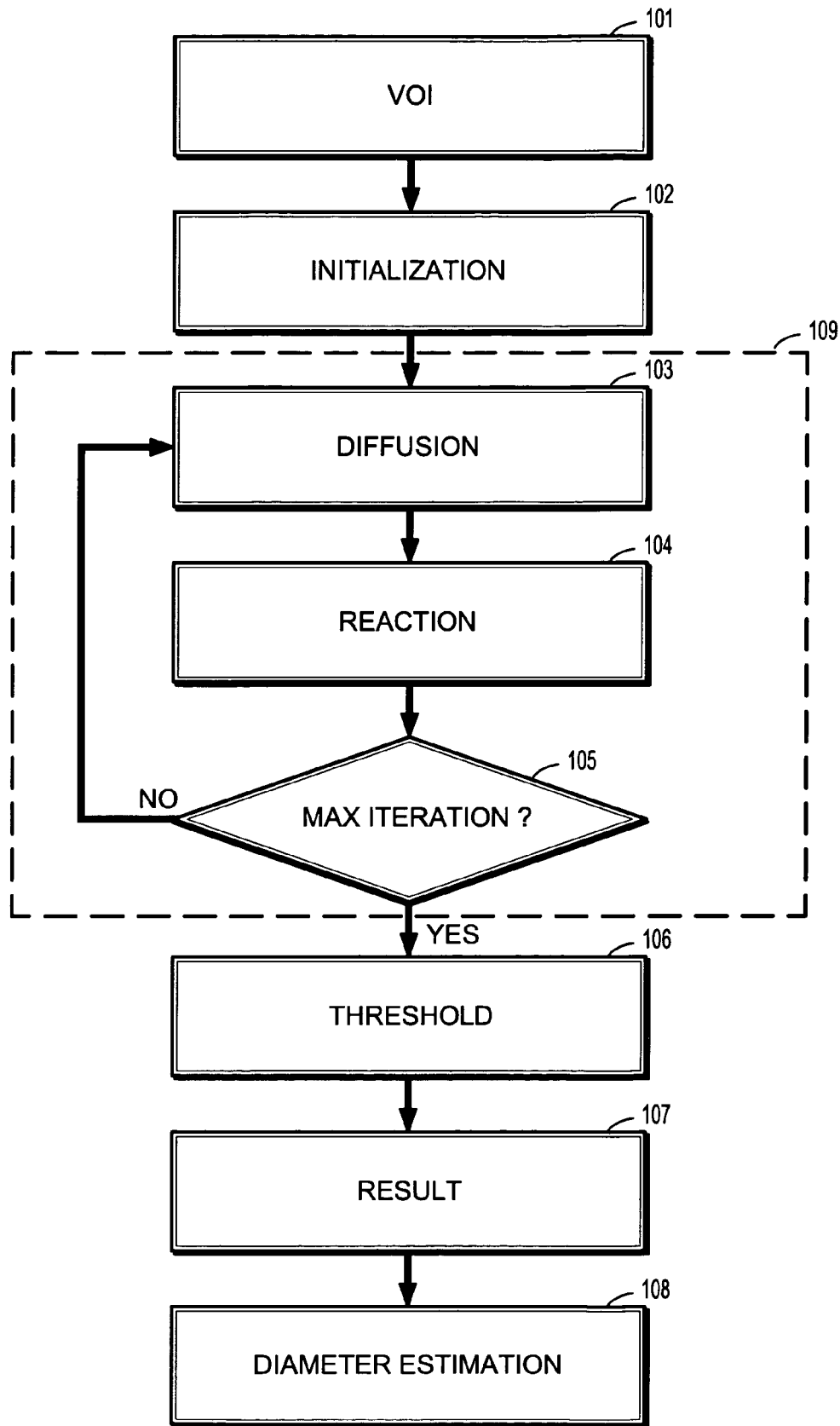
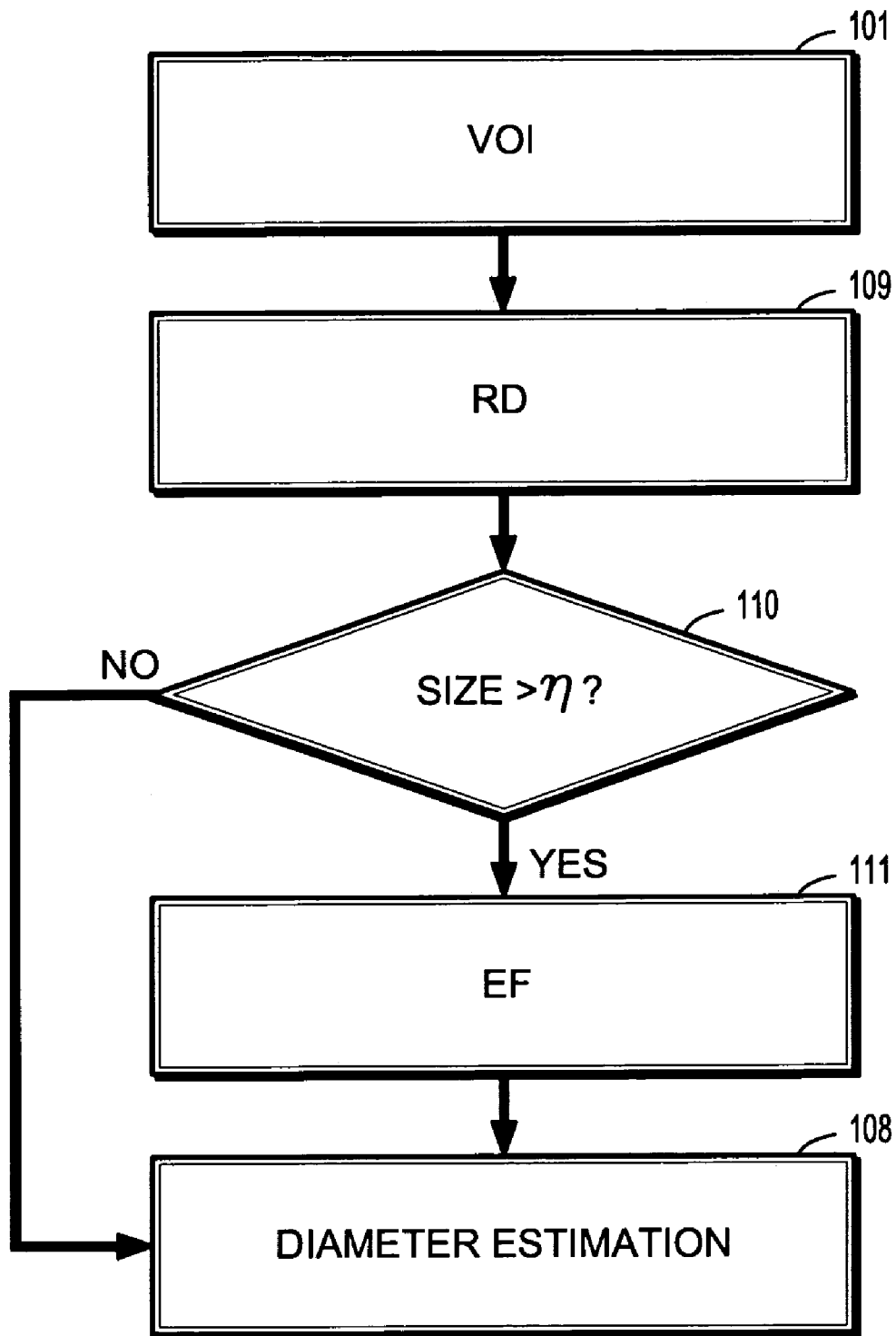


FIG. 1A



**FIG. 1B**

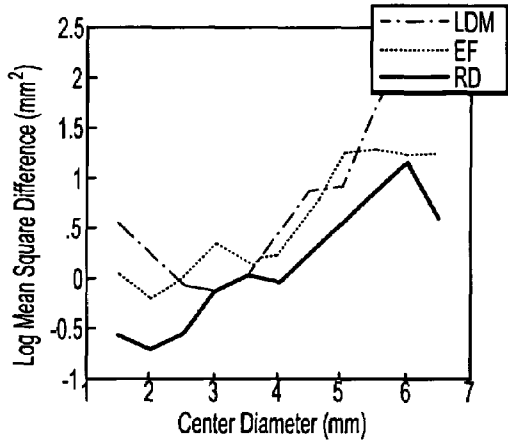


FIG. 2A

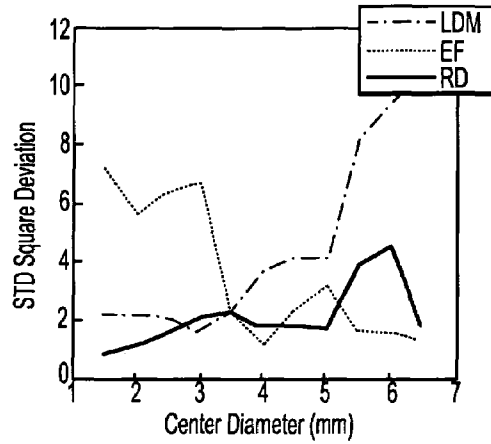


FIG. 2B

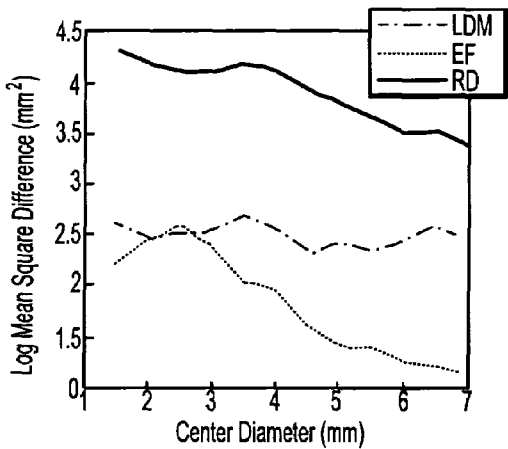


FIG. 3A

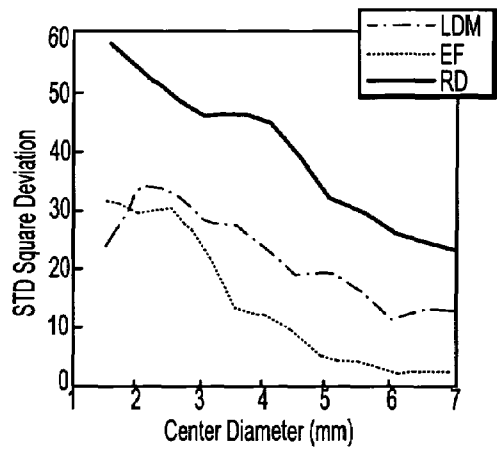


FIG. 3B

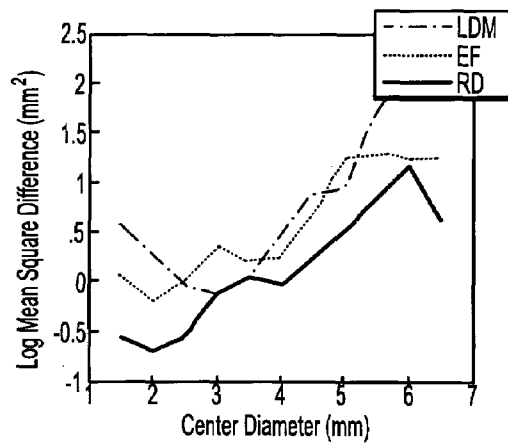


FIG. 4A

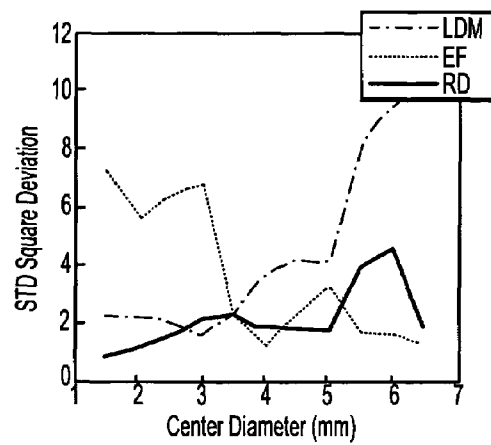


FIG. 4B

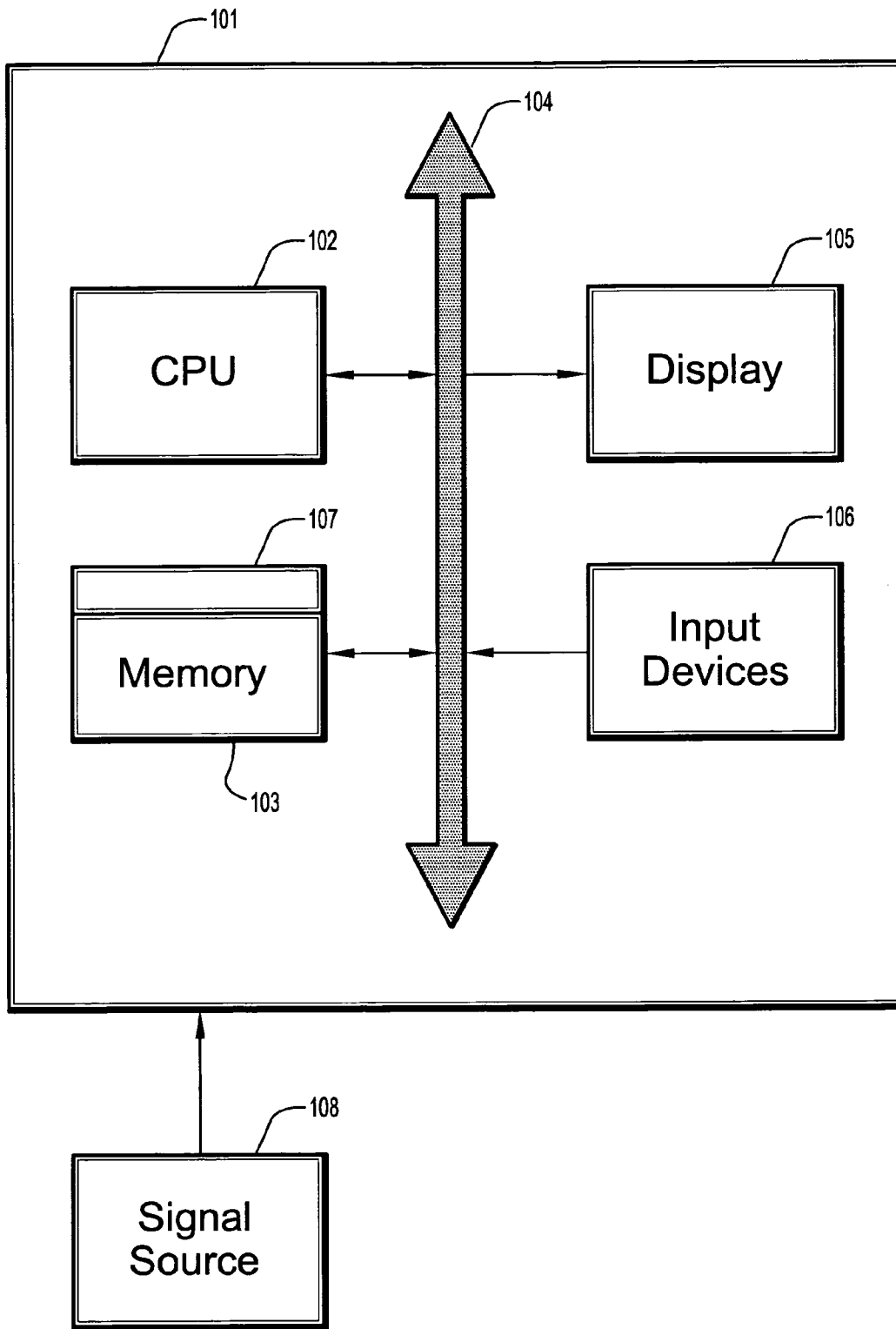


FIG. 5

# ESTIMATION OF SOLITARY PULMONARY NODULE DIAMETERS WITH A HYBRID SEGMENTATION APPROACH

## CROSS-REFERENCE TO RELATED APPLICATIONS

This application claims the benefit of Provisional Application No. 60/669,438 filed on Apr. 8, 2005 in the United States Patent and Trademark Office, the contents of which are herein incorporated by reference in its entirety.

## BACKGROUND OF THE INVENTION

### 1. Field of the Invention

The present disclosure relates to image processing, and more particularly to a system and method for estimating a size of solitary objects in of interest in medical images.

### 2. Description of Related Art

Measuring the size of pulmonary nodules from X-ray computed tomography (CT) data is an important practice for diagnosis and progression analysis of lung cancer. The nodule size often plays an important role in choosing a proper patient care, and is also an effective feature to separate true nodules from nodule-like spurious findings. Typically, the size is represented by the diameter of the nodule. Automating this task for computer-aided diagnosis (CAD) is, however, a difficult problem due to intensity variations, partial volume effects, attachment to other structures, and noises.

A Ct-based screening protocol specified by the International Early Lung Cancer Action Program (I-ELCAP) details how the diameter of pulmonary nodules should be measured and how the measurements should be used for determining the patient management. According to the protocol, the result of an initial CT screening of lung is considered positive if at least one solid or part-solid nodule with 5.00 mm or more in diameter or at least one non-solid nodule with 8.0 mm or more in diameter is found. Although these 5 mm and 8 mm thresholds are likely to drop as more accurate screening becomes possible with high resolution multi-detector helical CT (MDCT), the importance of module size in cancer diagnosis will stay unchanged.

To this end, an automated size estimation algorithm using a Gaussian Ellipsoid Fit (EF) has been developed. Given a marker positioned near a nodule, the algorithm computes the location, orientation and radii of an ellipsoid that models closely the intensity variation nearby the marker. It employs mean-shift and scale estimator to find the solution. The volume and diameter of the nodule can be estimated from the ellipsoid. EF can be incorporated into a CAD system where markers and provided from either manual markings of a reader or the detection algorithm of the system. The accuracy of the estimates has been verified using a large database with manual size measurements. However, the technique tends to have difficulties with small nodules due mainly to the small sample size problem.

## SUMMARY OF THE INVENTION

According to an embodiment of the present disclosure, a method for estimating a diameter of an object of interest, includes providing a volume of interest comprising a marker identifying a location of the object of interest, extracting a sub-volume of voxels around the marker, and initializing at least two volumes of the sub-volume, wherein each of the voxels has at least two values corresponding to the at least two volumes, respectively. The method includes performing,

iteratively, a diffusion operation and a reaction operation on the voxels to update at least two values, and comparing, for each voxel, the at least two values to a threshold to assign each voxel to one of the at least two volumes, wherein the assignment of the voxels is a segmentation result. The method further includes performing a boundary check to determine whether the object of interest is solitary, estimating a diameter of the object of interest from the segmentation result upon determining the object of interest to be solitary, and extracting the object of interest by performing ellipsoid fit on the sub-volume and estimating a diameter of the object of interest upon determining the object of interest to be non-solitary.

## BRIEF DESCRIPTION OF THE DRAWINGS

Preferred embodiments of the present invention will be described below in more detail, with reference to the accompanying drawings:

FIG. 1 is a flow chart according to an embodiment of the present disclosure;

FIGS. 2A-B are graphs of an estimate of performance of EF, LDM, and RD for solitary nodules according to an embodiment of the present disclosure;

FIG. 3A-B are graphs of an estimate of performance of EF, LDM, and RD for non-solitary nodules according to an embodiment of the present disclosure;

FIG. 4A-B are graphs of an estimate of performance of EF, LDM, and RD for solitary and non-solitary nodules according to an embodiment of the present disclosure;

FIG. 5 is a diagram of a computer system for implementing a method according to an embodiment of the present disclosure.

## DETAILED DESCRIPTION OF PREFERRED EMBODIMENTS

According to an embodiment of the present disclosure, a method for extracting a pulmonary nodule and estimating its diameter from helical thoracic CT scans. A rough location of the nodule is assumed to be given by either a reader or a computer aided diagnosis program. A combination of two segmentation methods: reaction-diffusion system (RD) and ellipsoid fit (EF) may be implemented. RD is used on solitary nodules and EF of non-solitary nodules. The solitary/non-solitary nodule type is determined with manual measurements of over 1300 nodules taken over 240 CT volumes. The performance of the hybrid approach is compared with a local density maximum algorithm, RD, and EF. The experiments show that the hybrid technique provides the most accurate size estimates, and reduces the computation time of EF by 50%.

### Segmentation

Referring to FIG. 1, according to an embodiment of the present disclosure, a reactive-diffusion system implements a segmentation algorithm that labels each voxel of an inputted volume of interest (VOI) (see block 101) to either foreground or background. Although a system may implemented more than two labels, the discussion is of a two-label system for simplicity. With RD segmentation, each voxel of the input volume to the segmentation accompanies two values:  $x_0(s)$  and  $x_1(s)$  where  $s$  denotes the location of the voxel. They take continuous values with the following constraints:  $x_0(s) \geq 0$ ,  $x_1(s) \geq 0$ , and  $x_0(s) + x_1(s) = 1$  for all  $s$ . These are background and foreground labels, respectively. A set of background labels forms a background volume, and a set of foreground labels forms a foreground volume.

The background and foreground volumes are initialized at block **102**. The initialization scheme is task dependent, and for the nodule segmentation task, we choose the following formula for each label.

$$x_1(1) = e^{-2(1 - \min(I(s)/1000))^2} \quad (1)$$

and  $x_0(s) = 1 - x_1(s)$  where  $I(s)$  denotes the CT value of the input volume at the locations  $s$ , and 1000 is near the upper CT value of non-calcified pulmonary nodules. Hence for voxels with  $I \geq 1000$ ,  $x_1 = 1$  and  $x_0 = 0$ . For voxels with  $I < 1000$ ,  $x_1$  decreases monotonically as  $I$  deviates from 1000 while  $x_0$  increases.  $x_1$  takes the minimum value of  $e^{-2}$  when  $I = 0$ .

After the initialization **102**, the background and foreground volumes undergo diffusion **103** and reaction **104** phases alternately for a number of times. During the diffusion phase, these volumes are diffused separately over the spatial domain. A linear diffusion **103** may be used, such as,

$$x_i \dot{Y}(s) = \lambda \nabla^2 x_i(s) \quad (2)$$

where  $i \in \{0, 1\}$  and the diffusion rate  $\lambda$  is set to 0.5.

During the reaction phase **104**,  $x_0(s)$  and  $x_1(s)$  compete against each other. The competition is implemented in a form of replicator dynamics as shown below.

$$x_i \dot{Y}(s) = \mu x_i(s) ((Ax(s))_i - x^T(s) Ax(s)) \quad (3)$$

where  $i \in \{0, 1\}$ ,  $x(s) = (x_0(s) x_1(s))^T$ ,  $\mu$  is the reaction rate,  $(Ax(s))_i$  denotes  $i$ th row of  $Ax(s)$ , and  $A$  is a fitness matrix. For experiments, a  $2 \times 2$  identity matrix was used as  $A$ . More complex matrices may be used for other tasks. The update rate is set to  $x(s)^T Ax(s)^{-1}$ . Then,

$$x_i(s) = x_i(s) (Ax(s))_i (x^T(s) Ax(s))^{-1} \quad (4)$$

The above replicator dynamics make sure that  $x_0 \geq 0, x_1 \geq 0$ , and  $x_0 + x_1 = 1$ , and constantly increases the average fitness value until it reaches the local maximum where each label becomes either 0 or 1. The diffusion process **103** encourages spatial homogeneity and adds disturbance to break a tie in the reaction phase **104**. After a few iterations, the outcome of the competition becomes clear and thresholding can be applied **106** at 0.5 on  $x_1$  to obtain the segmentation result **107**. In experiments the diffusion and the reaction phases were applied alternatively for four iterations **105**. Other numbers of iterations may be implemented.

According to an embodiment of the present disclosure, a Gaussian ellipsoid fit (EF) system implements a method which, given a marker positioned near a target nodule, fits a 3D anisotropic Gaussian function to the nodule's intensity distribution in a multiscale fashion. An ellipsoid that approximates the nodule's boundary is derived as a specific equal-probability contour of the fitted Gaussian. Various nodule size features (e.g., maximum diameter, volume, sphericity) are determined analytically from radii of the ellipsoid. The multiscale analysis is given by considering a Gaussian scale space in an increasing order, performing a Gaussian model fitting at each analysis scale, and find the most stable estimate among the multiscale estimates by minimizing a form of Jensen Shannon divergence criterion. At each scale, Gaussian mean as the nodule center location is estimated by the convergence of the scale mean shift procedures. In the neighborhood of the estimated mean, local data analysis is performed by the mean shift procedures initialized at a set of neighboring points. Gaussian covariance matrix as the anisotropic spread is estimated by the constrained least-squares solution of a linear system constructed with the convergent mean shift vectors. Parameter settings may be selected and varied depending on

an application. For example, for the experiments described herein, the scale space is conceived with 18 analysis scales with 0.25 interval  $(0.5^2, \dots, 4.75^2)$ . And 35% 3D confidence ellipsoid is used for deriving an equal-probability contour from the fitted Gaussian.

The local distribution maximum applies thresholding at multiple levels followed by connected component analysis on each thresholded volume. It then searches for object and their plateaus in the multiple thresholded volumes sequentially, starting from the one with the highest threshold value in the order of descending threshold values. A new object is found when a connected component has no overlaps to components in the previous volume. An object becomes a plateau when the ratio between the volume of the object and the volume of its bounding box suddenly decreases by more than some fraction (e.g.,  $\eta$ ) or the object merges with another plateau. Parameters of the method include the threshold values and  $\eta$ .  $\eta$  was set to  $1/30$  and the threshold levels were set to 0, 100, 200,  $\dots$ , 1100. Other parameter values may be selected.

The I-ELCAP protocol may be implemented for diameter estimation, wherein the diameter of a nodule is estimated as the average length and width where length is measured on a single CT image that shows the maximum length from among a plurality of segments of a segmentation; and width is defined as the longest perpendicular to the length of a segment having the maximum length. The CT image is selected along the axial direction, due to high-resolution and isotropic nature of the axial view. The I-ELCAP protocol may be implemented to estimate the diameter from the segmentation. Other measures of diameter may be implemented.

For LDM and RD, the diameter of a nodule is estimated as follows. After the segmentation and connected component analysis, the component that is closest to the marker is selected as the one corresponding to the nodule at the marker. In most cases, the marker is contained within the component, but in some cases, it points to the background due to inaccuracy in marker positioning. Next, the component is analyzed slice by slice in the axial view. For each axial slice, 2D connected component analysis is performed, an ellipse is fitted to each component, and the geometrical mean of the axes is recorded for each ellipse. Among all 2D connected components, we select the one with the maximum geometrical mean for diameter measurement. The diameter is then estimated as the average width and height of the bounding box enclosing the selected component. Use of the geometrical mean instead of the arithmetic mean gives a slightly better agreement with the manual measurements.

For EF, the diameter is estimated as follows. First, an ellipsoid directly derived from the estimated covariance is projected on the axial plane, and the radii of the ellipse on the projection plane is determined. The diameter can be estimated, for example, as the arithmetic mean of the radii times the scaling constant of 1.6416 corresponding to the 35% confidence limit.

Referring to FIG. 1B, according to an embodiment of the present disclosure, for a hybrid method, when a nodule is attached to another structure, RD segments both the nodule and structure together, resulting in a large volume. This segmentation volume usually stretches out to the boundary of the bounding volume ( $21 \times 21 \times 21$  in our experiments). This observation leads to a test for the nodule type: if the segmentation volume touches one of six boundaries of the bounding volume, it is considered non-solitary. Otherwise, it is considered solitary. The ratio between the segmentation volume and the volume of the bounding box enclosing the segmentation is determined to check if the segmentation has a reasonably



5

spherical shape. In experiments, only the boundary check was used to determine if the nodule is solitary.

By using this solitary/non-solitary check of a nodule with RD segmentation, a hybrid approach to the diameter estimation problem can be implemented. For each given marker of a VOI **111**, a sub-volume of  $21 \times 21 \times 21$  voxels were extracted, and RD segmentation **112** is applied to the volume. A boundary check **113** is applied to the segmentation **112** if the boundary check indicates the nodule to be solitary, a diameter estimation **115** is applied on the RD segmentation **112**. Otherwise, EF **114** is applied on the sub-volume and the diameter is estimated **115**. This hybrid approach is denoted HB.

Referring now to the experiments discussed herein; the performance of HB has been evaluated in estimating the diameter of pulmonary nodules. HB has been compared against EF, LDM and RD. Centered at each marker placed by radiologists near a pulmonary nodule, a  $21 \times 21 \times 21$  bounding volume was extracted and used as an input to the segmentation processes.

EF has difficulties in processing small nodules as the sample size for the estimate is small. EF can also mistakenly include surrounding background for the estimate, which leads to overestimate of the diameter.

A problem associated with LDM is its sensitivity to the pre-determined threshold levels, which are typically set by a fixed increment. The segmentation of an object becomes inaccurate when the intensity distribution of the object has an overlap with the distribution of its plateau. The degree and the frequency of the problem can be reduced by increasing the number of threshold levels, but at the cost of increasing the computational load.

RD is effective in estimating the diameter of solitary nodules.

The accuracy of the estimates were evaluated quantitatively by comparing them with manual measurements by human experts (both radiologists and scientists in the medical imaging field). We use 1349 nodules taken from over 240 CT volumes for the evaluation. The 1349 nodules are divided into 614 solitary and 735 non-solitary ones using the boundary test with the RD segmentation. The performance of EF, LDM, and RD were evaluated on solitary and non-solitary nodules separately. The accuracy is measured by the squared difference between estimates and the corresponding manual measurements. FIGS. 2 and 3 show the results for solitary and non-solitary nodules, respectively. In the plot, the mean and standard deviation of the squared difference errors are evaluated among nodules whose manual measurements are within  $\pm 0.5$  of the center diameter (placed at a 0.5 mm increment between 1.0 and 7.0). The mean is shown in log scale to improve the visibility of the data while the deviation is shown in linear scale. The purpose is to analyze the performance in terms of the nodule diameter.

For solitary nodules, the error tends to increase with the center diameter of the analysis. This, it is more informative to compare the results with the error normalized by the center diameter. RD is more accurate than EF and LDM across all sizes except at 3 mm where LDM with 0.2913 normalized error is slightly better than RD with 0.2972 normalized error. For non-solitary nodules, RD is the least accurate and EF is the most accurate one. For EF and RD, the error tends to decrease with the center diameter, while for LDM, it stays around  $2.5 \text{ mm}^2$ . The error on RD clearly comes from segmentation of both nodule and an attached structure.

The performance of HB was evaluated using all 1349 nodules. FIG. 4 shows the mean and the standard deviation of the squared difference error for EF, LDM and HB collected within the same diameter ranges as in FIGS. 2 and 3. Both

6

mean and deviation are shown in linear scale. HB constantly gives a smaller error than other methods in all sizes. This is predicted as HB uses RD and EF for solitary and non-solitary nodules, respectively, and the accuracy of RD and EF in their respective categories has been verified. Table 1 shows the mean and standard deviation of the computation time for each estimation technique. As shown, RD is computationally most efficient while EF is computationally most expensive. HB is about 50% faster than EF.

TABLE 1

	Computational Time (seconds)			
	METHOD			
	EF	LDM	RD	HB
Mean	1.26	0.269	0.0510	0.651
Std. Dev.	0.25	0.18	0.014	0.7

It is to be understood that the present invention may be implemented in various forms of hardware, software, firmware, special purpose processors, or a combination thereof. In one embodiment, the present invention may be implemented in software as an application program tangibly embodied on a program storage device. The application program may be uploaded to, and executed by, a machine comprising any suitable architecture.

Referring to FIG. 5, according to an embodiment of the present disclosure, a computer system **501** for implementing a method for estimating solitary pulmonary nodule diameters with a hybrid segmentation can comprise, inter alia, a central processing unit (CPU) **502**, a memory **503** and an input/output (I/O) interface **504**. The computer system **501** is generally coupled through the I/O interface **504** to a display **505** and various input devices **506** such as a mouse and keyboard. The support circuits can include circuits such as cache, power supplies, clock circuits, and a communications bus. The memory **503** can include random access memory (RAM), read only memory (ROM), disk drive, tape drive, etc., or a combination thereof. The present invention can be implemented as a routine **507** that is stored in memory **503** and executed by the CPU **502** to process the signal from the signal source **508**. As such, the computer system **501** is a general-purpose computer system that becomes a specific purpose computer system when executing the routine **507** of the present invention.

The computer platform **501** also includes an operating system and microinstruction code. The various processes and functions described herein may either be part of the microinstruction code or part of the application program (or a combination thereof), which is executed via the operating system. In addition, various other peripheral devices may be connected to the computer platform such as an additional data storage device and a printing device.

It is to be further understood that, because some of the constituent system components and method steps depicted in the accompanying figures may be implemented in software, the actual connections between the system components (or the process steps) may differ depending upon the manner in which the present invention is programmed. Given the teachings of the present disclosure provided herein, one of ordinary skill in the related art will be able to contemplate these and similar implementations or configurations.

Having described embodiments for a system and method for estimating solitary pulmonary nodule diameters with a hybrid segmentation, it is noted that modifications and varia-

7

tions can be made by persons skilled in the art in light of the above teachings. It is therefore to be understood that changes may be made in embodiments of the present disclosure that are within the scope and spirit thereof.

What is claimed is:

1. A computer-implemented method for estimating a diameter of an object of interest, comprising: a computer to implement the steps of:

providing a volume of interest comprising a marker identifying a location of the object of interest;

extracting a sub-volume of voxels around the marker; initializing at least two volumes of the sub-volume, wherein each of the voxels has at least two values corresponding to the at least two volumes, respectively;

performing, iteratively, a diffusion operation and a reaction operation on the voxels to update at least two values;

comparing, for each voxel, the at least two values to a threshold to assign each voxel to one of the at least two volumes, wherein the assignment of the voxels is a segmentation result;

performing a boundary check to determine whether the object of interest is solitary;

estimating a diameter of the object of interest from the segmentation result upon determining the object of interest to be solitary; and

extracting the object of interest by performing ellipsoid fit on the sub-volume and estimating a diameter of the object of interest upon determining the object of interest to be non-solitary.

2. The computer-implemented method of claim 1, wherein the ellipsoid fit is a Gaussian method.

3. The computer-implemented method of claim 1, wherein if the segmentation result touches one of six boundaries of the sub-volume, it is defined as non-solitary.

4. The computer-implemented method of claim 1, further comprising determining a ratio between the segmentation result and a volume of the sub-volume enclosing the segmentation result to determine if the segmentation has a reasonably spherical shape.

5. The computer-implemented method of claim 1, wherein the at least two volumes include a foreground volume and a background volume.

6. The computer-implemented reactive-diffusion method of claim 5, wherein the at least two values correspond to a foreground label and a background label, respectively.

7. The computer-implemented method of claim 1, wherein a number of iterations of the performing of the diffusion and reaction operations is predetermined.

8

8. The computer-implemented method of claim 1, wherein performing the diffusion operation comprises performing a linear diffusion.

9. The computer-implemented reactive-diffusion method of claim 8, wherein the linear diffusion is given by  $x_i \dot{Y}(s) = \lambda \nabla^2 x_i(s)$ , where  $i \in \{0, 1\}$  and the diffusion rate  $\lambda$  is set to 0.5.

10. The computer-implemented method of claim 1, wherein performing the reaction operation comprises performing a competition between the at least two values in a form of replicator dynamics implementing a fitness matrix, wherein the replicator dynamics updates the at least two values.

11. The computer-implemented reactive-diffusion method of claim 10, wherein performing the reaction operation comprises enforcing that each of the at least two values is greater than or equal to zero and the sum of the at least two values is one.

12. The computer-implemented reactive-diffusion method of claim 11, wherein the diffusion operation adds disturbance to break a tie between the at least two values in the reaction operation.

13. A computer storage medium readable by a computer, tangibly embodying a program of instructions executable by the computer to perform method steps for estimating a diameter of an object of interest, the method steps comprising:

providing a volume of interest comprising a marker identifying a location of the object of interest; extracting a sub-volume of voxels around the marker; initializing at least two volumes of the sub-volume, wherein each of the voxels has at least two values corresponding to the at least two volumes, respectively; performing, iteratively, a diffusion operation and a reaction operation on the voxels to update at least two values; comparing, for each voxel, the at least two values to a threshold to assign each voxel to one of the at least two volumes, wherein the assignment of the voxels is a

segmentation result; performing a boundary check to determine whether the object of interest is solitary; estimating a diameter of the object of interest from the segmentation result upon determining the object of interest to be solitary; and extracting the object of interest by performing ellipsoid fit on the sub-volume and estimating a diameter of the object of interest upon determining the object of interest to be non-solitary thus reducing the diameter estimation bias that is introduced with small dimensions modules.

\* \* \* \* \*